Behavioral/Systems/Cognitive

Spatiotemporal Receptive Fields of Peripheral Afferents and Cortical Area 3b and 1 Neurons in the Primate Somatosensory System

Arun P. Sripati,[1,2] Takashi Yoshioka,[1,3] Peter Denchev,[1] Steven S. Hsiao,[1,3,4] and Kenneth O. Johnson[1,3,4]

[1]Zanvyl Krieger Mind/Brain Institute and Departments of [2]Electrical and Computer Engineering, [3]Neuroscience, and [4]Biomedical Engineering, Johns Hopkins University, Baltimore, Maryland 21218

Neurons in area 3b have been previously characterized using linear spatial receptive fields with spatially separated excitatory and inhibitory regions. Here, we expand on this work by examining the relationship between excitation and inhibition along both spatial and temporal dimensions and comparing these properties across anatomical areas. To that end, we characterized the spatiotemporal receptive fields (STRFs) of 32 slowly adapting type 1 (SA1) and 21 rapidly adapting peripheral afferents and of 138 neurons in cortical areas 3b and 1 using identical random probe stimuli. STRFs of peripheral afferents consist of a rapidly appearing excitatory region followed by an in-field (replacing) inhibitory region. STRFs of SA1 afferents also exhibit flanking (surround) inhibition that can be attributed to skin mechanics. Cortical STRFs had longer time courses and greater inhibition compared with peripheral afferent STRFs, with less replacing inhibition in area 1 neurons compared with area 3b neurons. The greater inhibition observed in cortical STRFs point to the existence of underlying intracortical mechanisms. In addition, the shapes of excitatory and inhibitory lobes of both peripheral and cortical STRFs remained mostly stable over time, suggesting that their feature selectivity remains constant throughout the time course of the neural response. Finally, the gradual increase in the proportion of surround inhibition from the periphery to area 3b to area 1, and the concomitant decrease in response linearity of these neurons indicate the emergence of increasingly feature-specific response properties along the somatosensory pathway.

Key words: **receptive field; somatosensory cortex; macaque; spatial transformations; peripheral nerve; tactile**

Introduction

The long-term objective of this research is to characterize the neural representation of spatial form along the somatosensory pathway. In the periphery, information about spatial form and motion is conveyed by slowly adapting (SA1) and rapidly adapting (RA) afferents (Johnson, 2001). This peripheral afferent information reaches the cortex, where it is first processed by areas 3b, 1, and 2 (Jones and Powell, 1970). In this study, we recorded from peripheral SA1 and RA afferents and from neurons in cortical areas 3b and 1, using identical stimuli. We then estimated their spatiotemporal receptive fields (STRFs), which characterize the neural responses as a linear summation of the tactile stimulus along both spatial and temporal dimensions.

The spatial and temporal features of the STRFs from a given anatomical area were then compared with the known functional properties of these neurons, which are briefly reviewed below. In the periphery, SA1 afferents have small receptive fields and sustained responses to steady indentations, whereas RA afferents have larger receptive fields and transient responses to indentation onset and withdrawal (Johnson, 2001). Evidence suggests that SA1 and RA afferents are responsible for different aspects of tactile perception (Johnson, 2001). Responses in cortex are considerably more complex compared with the periphery. Compared with neurons in area 3b, area 1 neurons are known to have larger receptive fields often spanning multiple digits (Hyvärinen and Poranen, 1978; Vierck et al., 1988; Iwamura et al., 1993). There is considerable variance in the literature regarding other functional differences between areas 3b and 1; some studies report no significant differences (Mountcastle and Powell, 1959; Darian-Smith et al., 1984), whereas others report that area 1 neurons have slightly longer latencies (Lebedev and Nelson, 1996), greater surround inhibition (Sur et al., 1980), more complex responses to scanned letters (Phillips et al., 1988), and are less slowly adapting (Prud'homme et al., 1994). Neurons from both areas 3b and 1 exhibit orientation selectivity (Pubols and LeRoy, 1977; Gardner, 1988; Hsiao et al., 2002), although there is evidence for greater orientation selectivity in area 3b and greater motion selectivity in area 1 (Warren et al., 1986).

Previous studies have shown that spatial receptive fields account reasonably well for the responses of area 3b neurons to scanned spatial stimuli (DiCarlo et al., 1998; DiCarlo and John-

Received Sept. 2, 2005; revised Jan. 5, 2006; accepted Jan. 6, 2006.

This work was supported by National Institutes of Health Grants NS38034 and NS18787. We thank Justin Killebrew and Frank Dammann for technical support and Sara Szczepanski, Jeff Lawson, Sliman Bensmaia for help with collecting the neurophysiological data. Bill Nash and Bill Quinlan assisted with designing equipment necessary for the recordings.

Correspondence should be addressed to Steven S. Hsiao, Zanvyl Krieger Mind/Brain Institute, Johns Hopkins University, 3400 North Charles Street, Baltimore, MD 21218. E-mail: Steven.Hsiao@jhu.edu.

DOI:10.1523/JNEUROSCI.3720-05.2006

 0270-6474/06/262101-14$15.00/0

son, 1999; DiCarlo and Johnson, 2000). However, the temporal relationships between excitation and inhibition, as well as the extent to which these properties vary across anatomical areas are unknown. Here, we expand on previous studies and describe receptive fields with spatial as well as temporal modulations. The parameters of these spatiotemporal receptive fields are estimated using standard reverse correlation methods (de Boer and Kuyper, 1968; Aertsen and Johannesma, 1981; Palmer and Davis, 1981; DeAngelis et al., 1995; DiCarlo et al., 1998). We then characterize the spatial structure and relative timing of excitation and inhibition in the STRFs. The results suggest a gradual transformation of tactile information from the periphery to area 3b and then to area 1.

Materials and Methods

Eight macaque monkeys (*Macacca mulatta*; 4–9.5 kg) were used in this study: six anesthetized monkeys in the peripheral nerve experiments, and two awake, behaving monkeys in the cortical experiments. All experiments were performed in compliance with the guidelines of the Johns Hopkins University Animal Care and Use Committee and the National Institutes of Health *Guide for the Care and Use of Laboratory Animals*.

Peripheral experiments

Single unit recordings were made from the median and ulnar nerves of macaque monkeys using standard methods (Talbot et al., 1968). Briefly, animals were sedated with ketamine (20 mg/kg, i.m.) and anesthetized with Nembutal (sodium pentobarbital; 25 mg/kg, i.v.). Additional doses of Nembutal were used to keep the animals areflexic. A 2 inch incision was made on the upper or lower arm, and blunt dissection was used to isolate the ulnar or median nerve. A small bundle of axons was split repeatedly until a single afferent fiber was isolated using a time–amplitude window discriminator (model DIS-1; Bak Electronics, Mount Airy, MD). Recordings were performed only on afferents with receptive fields (RFs) located in the central portion of the distal fingerpad of digits 2–4 on either hand. Standard procedures were used to classify the afferent as SA1 or RA (Talbot et al., 1968). If the afferent responded with sustained firing in response to a continued indentation, it was classified as SA1; if it responded transiently to the onset and withdrawal of an indentation, it was classified as RA. Pacinian responses were not recorded, because they are insensitive to the spatial structure of the stimulus (Yoshioka et al., 2001).

Cortical experiments

Experimental methods were similar to those described previously (DiCarlo et al., 1998) and are described briefly here. Each monkey was trained to perform saccadic eye movements to a flashing spot of light displayed randomly at one of four corners on a computer screen. The animal was rewarded for correct responses with a drop of water (0.1 cc per correct trial) and was allowed to work until it was satiated (as indicated by its refusal to perform more trials). Once the animal learned the task with >80% success, a small craniotomy (~5–7 mm diameter) was made over the primary somatosensory cortex under ketamine anesthesia (20 mg/kg) with the dura left intact.

Electrophysiological recordings were made in the postcentral gyri using standard techniques (Mountcastle et al., 1991; DiCarlo et al., 1998). On each recording day, a multielectrode microdrive (Mountcastle et al., 1991) was loaded with seven quartz-coated platinum/tungsten (90/10) electrodes (diameter, 80 μm; tip diameter, 4 μm; impedance, 2–4 MΩ at 1000 Hz), aligned in a single row and separated by 400 μm. The microdrive proboscis was then inserted into a recording chamber filled with physiological saline and oriented so that the electrodes were normal to the skull. The electrodes were then driven into the cortex until they encountered neurons in area 1 with RFs on the distal finger pads. After recording from area 1, the electrodes were further advanced into area 3b. Because the electrodes were aligned perpendicular to the central sulcus, we could typically record from three to four electrodes that had RFs on the same fingerpad (Hsiao et al., 1996). The identification of areas 1 and 3b was accomplished in two ways: initially, during the experiments, by physiologically mapping RFs using handheld probes and later, after euthanasia, by anatomically identifying electrode tracks through histology (DiCarlo et al., 1996). We used the characteristic progression of RF locations from area 1 to area 3b to identify the cortical areas during the experiments (Merzenich et al., 1978; Sur et al., 1984). This progression was typical in all hemispheres; the superficial tissue of area 1 exhibited RF progressions of distal, middle, proximal finger pads, and then palmar whorls. As the electrodes moved further into area 3b, the proximal finger representation appeared, followed by receptive fields on the middle and distal fingerpads. We recorded only from neurons with RFs on distal fingerpads of digits 2–4 while stimulating the pad using a 400-probe array stimulator (see below). On each day of recording, the electrode array was shifted ~200 μm along the post-central gyrus until, after 20–30 d of recording in each hemisphere, almost the entire glabrous distal fingerpad representation of digits 2–4 was covered. All essential events during the experiments were stored in a computer with a temporal resolution of 0.1 ms; these events included stimulus location, probe amplitudes, and the times of occurrence of action potentials, as well as behavioral events. At the end of each recording day, the electrodes were withdrawn and a few drops of neomycin, polymixin B, and dexamethasone ophthalmic solution, and a drop of gentamicin ophthalmic solution were applied to the dura. The dura was then covered with Gelfoam, and the chamber was filled with sterile saline and sealed.

Recordings were obtained from neurons in areas 3b and 1 that met the following criteria: (1) the action potentials of the neuron were well isolated from the background noise, (2) the RF of the neuron included at least one of the distal fingerpads on digits 2–4, and (3) the stimulator array could be positioned so that the RF of the neuron was centered in the array. STRFs were estimated from a total of 257 neurons from cortical areas 3b and 1 across the two monkeys. Of these, 138 neurons were chosen for additional analysis based on the following criteria: (1) the evoked firing rates were stable throughout the recording, and (2) several of the estimated receptive field weights were significantly different from the background noise level (see below, STRF noise removal).

Receptive field areas on the hand. Before delivering the random indentation stimulus, the receptive field of each neuron was mapped manually with a punctate probe to determine the approximate size of the receptive field on the hand. Subsequent stimulation with the 400-probe stimulator (described below) only yielded the structure of the receptive field within a single fingerpad. Using manual probes, we found that 97% (56 of 58) of neurons in area 3b had RFs that were completely localized within a single fingerpad. The remaining 3% (2 of 58) neurons had RFs spanning multiple fingerpads within a single finger. In area 1, 34% (27 of 80) of the neurons had RFs restricted to a single fingerpad, 41% (33 of 80) of the neurons had RFs spanning multiple fingerpads in a single finger, and the remaining 25% (20 of 80) of the neurons had RFs spanning multiple digits. In the case of neurons with RFs spanning multiple digits, the stimuli were delivered to the distal fingerpad that was most responsive to handheld stimulation.

Four-hundred-probe array stimulator

A tactile stimulator consisting of 400 independently controlled probes arranged in a 20 × 20 array over a 1 cm^2 area was used to stimulate the distal fingerpad. The spacing between the probes exceeded the average spacing between afferent fibers of each type (Johnson, 2001). Each probe has a diameter of 0.3 mm, and the spacing between their centers is 0.5 mm. Probe amplitudes were measured every 2 ms using optical sensors with an accuracy of 2–5 μm. The rise time constant of the probes (in response to a step command) was 10 ms on average. For both peripheral and cortical experiments, the point of maximum sensitivity of the neuron was located using a handheld probe and marked on the skin using an ink pen, and the stimulator was centered on this point with a preindentation of 1 mm into the skin. We chose not to stimulate digit 5, because it is smaller than the other digits, causing it to have a smaller area of contact with the stimulator compared with digits 2–4. Contact areas for the other digits (2–4) were approximately equal.

Stimulus design

Spatiotemporal random indentation stimulus. The spatiotemporal random indentation (STRI) stimulus used in this study is an extension of the

scanned, embossed random dots used in previous studies (DiCarlo et al., 1998). Whereas these scanned random dots varied only along the spatial dimension, the STRI stimulus used here varies along both spatial and temporal dimensions. In this stimulus, each probe in the array began moving at random times according to an independent Poisson process with a specified rate. Each probe movement had an amplitude chosen uniformly at random between 0 and 500 μm and lasted for a fixed duration. The total number of probe movements per second (i.e., 400 times the indentation rate of each pin; called indentation density) could be set to a value between 90 and 2048 indentations per second. The movement of a single probe and its normalized spectrum are illustrated in Figure 1*C*.

Two slightly differing STRI protocols, denoted by A and B, were used in the peripheral and cortical experiments. In protocol A, the indentation density was fixed at 1024 indentations per second. Each probe indentation was trapezoidal with a duration of 30 ms (i.e., up-ramp, hold, and down-ramp periods were 10 ms each). The entire stimulus lasted 600 s. In protocol B, we determined the preferred indentation density for each neuron by running short (8 s) segments of stimuli with 10 different indentation densities (90, 128, 181, 256, 362, 512, 724, 1024, 1448, and 2048 indentations/s) and then chose the STRI stimulus with the density that evoked the maximum firing rate. The duration of each trapezoidal indentation in protocol B was reduced to 20 ms to minimize the effects of stimulus temporal autocorrelation on the receptive field (see below, Spatiotemporal receptive field estimation). Furthermore, the stimulus duration in protocol B was shortened to 200 s and repeated three times.

Punctate probe stimuli. In addition to the STRI protocol, we also used the 400-probe stimulator to record neural responses evoked by individual probe indentations across the entire array. Each probe indentation had an amplitude of 300 μm, lasted 100 ms, and was repeated five times. The increase in the response (from spontaneous activity levels) evoked by each probe was defined as the punctate probe receptive field.

Spatiotemporal receptive field estimation

The method used to estimate the spatiotemporal receptive field is a modification of methods previously reported by DiCarlo et al. (1998). The neural response is taken to be the mean firing rate in each 10 ms window, and the stimulus in each window is taken to be the mean probe amplitude.

Because neurons adapt to the overall stimulus intensity (Vega-Bermudez and Johnson, 1999a), we specified the stimulus in terms of deviations from its mean amplitude. Similarly, we specified the neural response at any time as the deviation from the average level of activity. This allowed us to characterize the modulations in firing rate rather than the overall level of activity. Note that subtracting the mean from the stimulus or the response does not affect the remaining linear weights, which make up the STRF of the neuron. Thus, for any stimulus, the STRF can be used to predict the deviation of the instantaneous response from the overall mean.

The firing rate of the neuron at any time step n is taken to be the spatiotemporal linear summation of the stimuli in the preceding 100 ms (i.e., over the previous 10 time samples). In other words,

$$r_n = \mathbf{S}_n\mathbf{b_0} + \mathbf{S}_{n-1}\mathbf{b_1} + \cdots + \mathbf{S}_{n-k}\mathbf{b_k} + \mathbf{S}_{n-9}\mathbf{b}_9,$$

where r_n is the response at time n, $\mathbf{S_n}$ is a 1×400 vector of the amplitudes of the 400 probes at time n, and $\mathbf{b_k}$ is a 400×1 vector containing the 400 weights that represent the contribution of the stimulus that occurred k time samples earlier to the current response. The vectors $\mathbf{b_0} \ldots \mathbf{b_9}$ together constitute the STRF of the neuron.

The set of responses (over all time instants) form a set of simultaneous equations that can be rewritten in matrix form as follows:

$$\mathbf{r} = \mathbf{Xb},$$

where $\mathbf{r}$ is the vector containing the responses at all time instants, $\mathbf{X}$ is the stimulus matrix, and $\mathbf{b}$ is the vector $[\mathbf{b_0} \ldots \mathbf{b_9}]$ (i.e., the concatenation of the spatial receptive fields at different delays). This matrix equation can be solved for $\mathbf{b}$ as follows:

$$\mathbf{b} = (\mathbf{X^T X})^{-1}\mathbf{X^T r}.$$

The matrix $\mathbf{X^T X}$ represents the spatiotemporal autocorrelation of the stimulus. An ideal white noise stimulus has no temporal or spatial correlation, making $\mathbf{X^T X}$ an identity matrix and the inversion trivial. In practice, the STRI stimulus had some temporal correlation (because probe movements have a nonzero duration) but no spatial correlation (because probes moved independently). The lack of spatial correlation implies that the contribution of each pin to the response can be estimated separately. Mathematically, this is equivalent to separating the spatial and the temporal components of the stimulus autocorrelation matrix. Thus, we computed the following for the *pth* pin:

$$\mathbf{b}_p = (\mathbf{X}_p^T\mathbf{X}_p)^{-1}\mathbf{X}_p^T\mathbf{r},$$

where the $\mathbf{X}_p$ matrix is the stimulus matrix for pin p alone and $\mathbf{b_p}$ is the vector of 10 weights for pin p.

Inverting the matrix $\mathbf{X}_p^T\mathbf{X}_p$ is equivalent to dividing the power spectrum of the reverse correlation ($\mathbf{X}_p^T\mathbf{r}$) at each frequency by its corresponding value in the stimulus power spectrum. If the stimulus is white, it would have equal power at all frequencies. However, because of temporal correlation in the stimulus, there is more power at low frequencies and little power at high frequencies. As a result, direct inversion of the $\mathbf{X}_p^T\mathbf{X}_p$ matrix amounts to dividing by quantities close to zero, magnifying the high-frequency components that are likely absent in the original receptive field. The natural solution is to take the pseudo-inverse of $\mathbf{X}_p^T\mathbf{X}_p$ using singular value decomposition and retain power at lower frequencies while ignoring power at high frequencies. The choice of which frequencies (or singular values) are significant involves a tradeoff: retaining all frequencies introduces large amounts of noise in the receptive field, whereas retaining few frequencies can affect the true temporal modulations of the receptive field. It must be noted that temporal autocorrelation effects can only be mitigated (but not removed) by using the pseudo-inverse, or by shortening the indentation waveform. For example, because the pin indentation was shortened from 30 to 20 ms in protocol B, there were fewer temporal autocorrelation effects in protocol B than in protocol A (see Discussion). Based on computer simulations using actual probe data, we retained singular values $>0.5\%$ of the maximum singular value for all neurons.

Static output nonlinearity

The description above assumes the neural response to be a linear spatiotemporal integration of the stimulus on the fingerpad. However, unlike a linear output, which can be both positive and negative, the neural response is always non-negative. Therefore, an additional transformation is needed to convert the linear output into the predicted (non-negative) firing rate. We therefore performed a half-wave rectification, a natural choice given the presence of a threshold in the neural response. In general, this transformation can be estimated by comparing the observed response with the linear prediction (Dayan and Abbott, 2001). However, we found no significant improvement in the STRF predictions obtained using a general polynomial transformation beyond the predictions obtained using half-wave rectification.

STRF noise removal

Determining which regions of the STRF are significant is important to obtain a reliable characterization of the features in the STRF. STRF estimates are noisy for two reasons: (1) because the STRI stimulus has a limited duration, the STRF computation yields an estimate of the true STRF. The noise in this estimate reduces with increasing stimulus duration; and (2) the neural response has an inherent trial-to-trial variability, causing random fluctuations in the estimated STRF. These fluctuations can be reduced by obtaining responses to multiple runs of the same stimulus and then using the mean response to compute the STRF. Given the limited recording duration, there is a tradeoff between the two sources. Based on computer simulations, we determined that the dominant source of variability in the STRF estimates was the overall duration of the STRI stimulus rather than the response variability.

Our procedure for removing noise pixels from the STRF is similar to the one used by DiCarlo et al. (1998) and is described briefly. STRFs were first convolved with a spatial Gaussian filter with SD of 300 μm. Next, we chose the noise level in the STRF as the SD of the STRF weights at the 100

ms lag, because STRFs rarely lasted longer than 80 ms. Weights whose magnitude was smaller than the noise level were then set to zero. To reduce the effect of noise on the measurements of area and mass, we required that every nonzero bin in the thresholded STRF have at least four neighboring bins that are also nonzero. All STRF properties reported here are based on this noise-removed STRF.

Results

STRI stimuli were presented to the receptive fields of 53 peripheral afferents (32 slowly adapting type 1; 21 rapidly adapting) across six anesthetized monkeys and 138 cortical neurons from areas 3b and 1 of the primary somatosensory cortex (58 from area 3b; 80 from area 1) from three hemispheres of two monkeys performing a visual task unrelated to the tactile stimulus. All recordings were obtained from neurons responsive to stimulation on the distal fingerpads of digits 2, 3, and 4. Stimuli were delivered using a 20 × 20 probe array spanning an area of 1 cm^2. Neurons were studied using two similar STRI protocols, A and B (see Materials and Methods). For clarity of presentation, the results below are shown primarily for responses to STRI protocol A; these include data from 31 peripheral afferents (16 SA1; 15 RA) and 77 cortical neurons from SI cortex (33 from area 3b; 44 from area 1). Portions of this work have appeared previously in abstract form (Yoshioka et al., 2002).

The results are organized as follows: First, we describe the typical STRFs observed in peripheral SA1 and RA afferents, and in neurons from area 3b and area 1. Then, we compare and describe the spatial and temporal characteristics of the population of STRFs from a given anatomical area. Finally, we examine several properties of the neural responses evoked by the STRI stimulus.

Typical STRFs

Figure 1*A* illustrates the STRF of a neuron from cortical area 3b. In Figure 1*A*, the STRF slice represents the contribution of the probe at each spatial location toward the response produced 15 ms after its indentation. Each pixel in the STRF represents a region of 0.25 mm^2, which is the area of skin below each probe in the stimulator array. An excitatory (inhibitory) weight implies that an indentation at that location will result in an increase (decrease) in firing relative to the mean response. We defined a complete STRF to be the set of STRF slices at all lags at which indentations evoked significant changes in the firing rate from the mean level.

The operation of the STRF is illustrated in Figure 1*B*, together with the predicted and observed responses during a short segment of the STRI stimulus. The movements of a typical probe during a 3 s time window are illustrated in Figure 1*C* along with its normalized power spectrum. In Figure 1*B*, the convolution of the STRF with the stimulus to produce the response is illustrated at two times, *t*1 and *t*2. The response at each time is produced by multiplying the stimulus amplitudes at each time lag (Fig. 1*B*, grayscale pixels) with the STRF weights at the corresponding lag (Fig. 1*B*, superimposed color pixels), and adding them together. For example, in Figure 1*B*, top panel (for $t = t1$), the probes in the stimulus tend to indent the excitatory region. As a result, the net

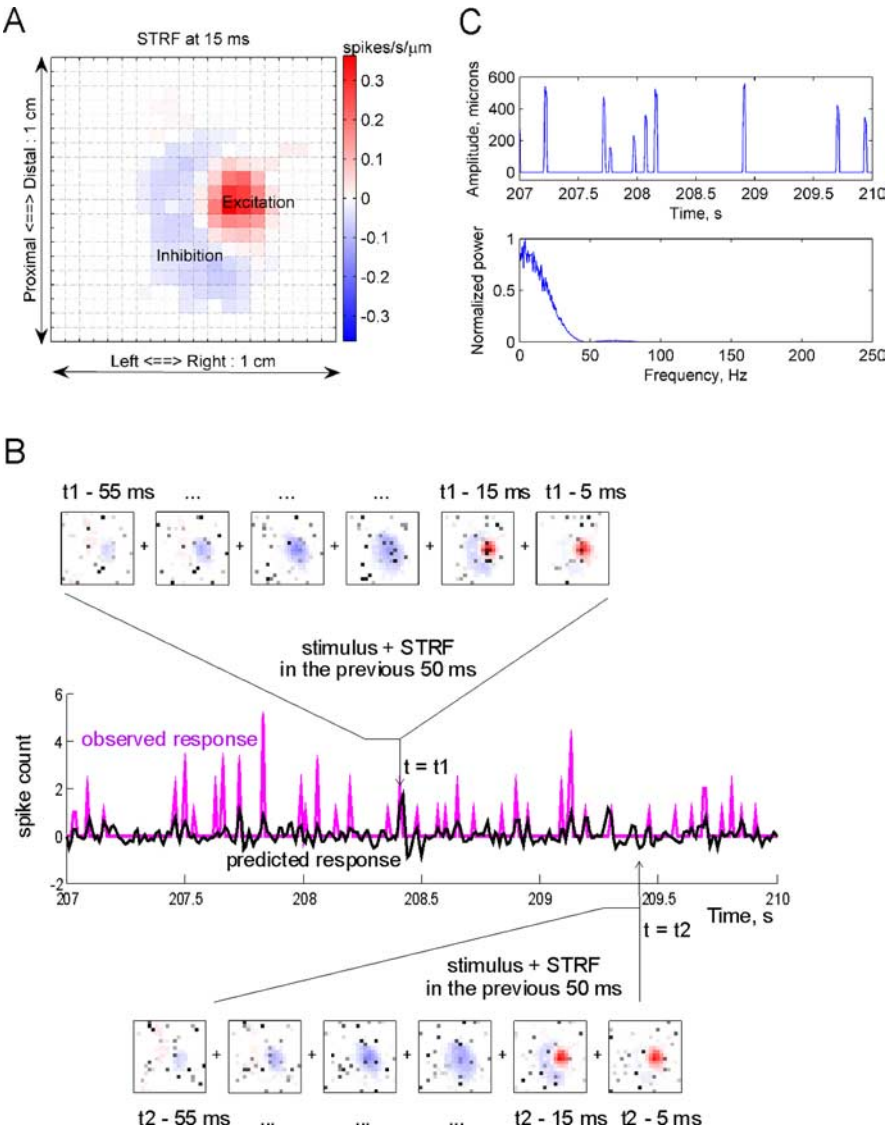

Figure 1. A typical STRF. ***A***, A single slice of the STRF from area 3b unit at $t = 15$ ms. Each pixel represents one probe in the 20 × 20 stimulator array, covering a 1 cm^2 area on the fingerpad (see Materials and Methods). The value at each probe location in the STRF slice indicates the change in firing rate per micrometer unit indentation (in spikes per second per micrometer) at time t_0 when a probe is indented at that location at time $t = t_0 - 15$ ms. Excitatory pixels are shown in red, and inhibitory pixels are shown in blue. The STRF is viewed as if looking down on the distal fingerpad, with the long axis of the finger pointing upward. ***B***, The middle panel depicts the evoked response to the STRI stimulus (magenta) and the linear prediction (black) of the STRF of the same area 3b neuron during a 3 s time window. The panels above and below illustrate the computation of the predicted response at two time instants indicated by the arrows. In each frame, the STRI stimulus (grayscale) is superimposed over the STRF (color; excitatory pixels in red; inhibitory pixels in blue). Darker grayscale pixels indicate larger indentations. The predicted response at time *t* is computed by taking the pixel-by-pixel product of the STRF at each instant with the corresponding stimulus frame, and summing the result over a 50 ms time window before time *t*. Top panel, An increase in firing rate is predicted by the STRF when the probes stimulate the excitatory region of the receptive field. Bottom panel, A decrease in firing rate is predicted when the probes stimulate the inhibitory region. ***C***, Top panel, Measured indentation amplitude versus time for a probe in the center of the excitatory region (11th row from top and 14th column from left) during a 3 s time window (identical to ***B***). Bottom panel, Normalized power spectrum for this probe computed over the duration of the entire stimulus.

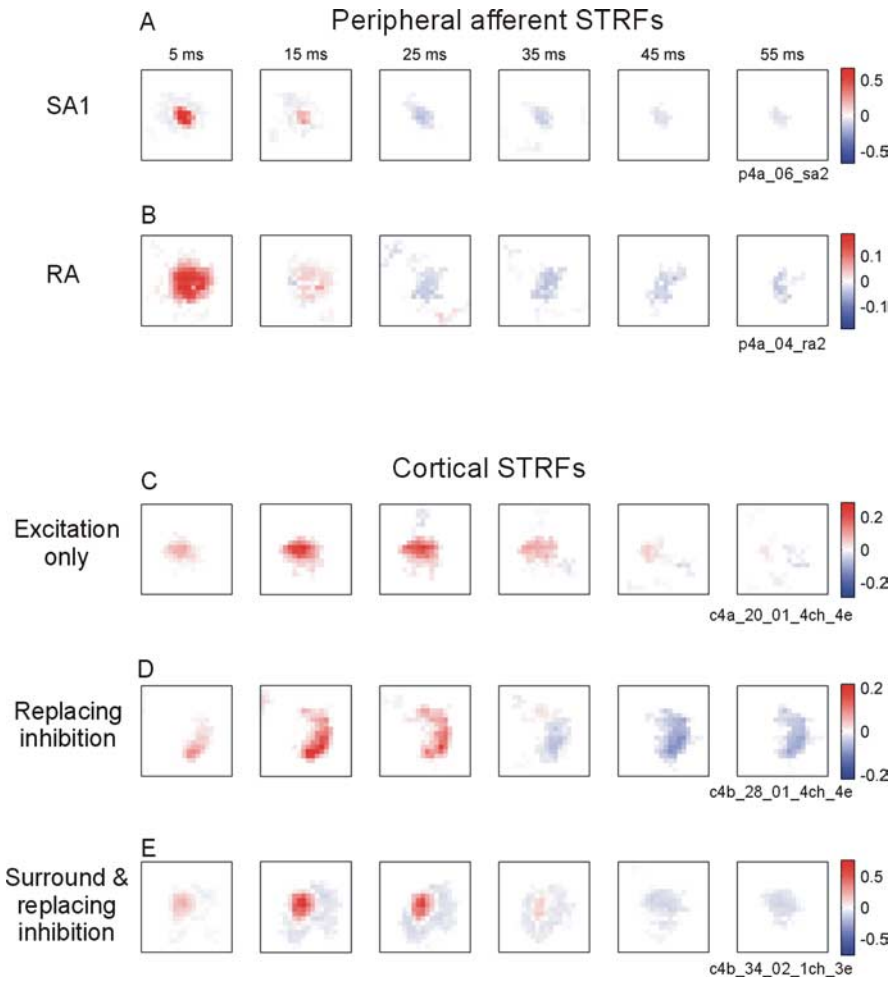

Figure 2. Typical peripheral and cortical STRFs. STRFs of a peripheral SA1 afferent (***A***) and a peripheral RA afferent (***B***). STRFs in primary somatosensory cortex (areas 3b and 1) could be broadly categorized into three types. ***C***, An area 3b unit with a purely excitatory STRF. ***D***, An area 3b unit with replacing inhibition. ***E***, An area 1 unit with surround and replacing inhibition. Color bars indicate pixel intensities in spikes per second per micrometer.

impact is a predicted increase in the response, in agreement with the observed spikes at $t = t1$. Similarly, in Figure 1*B*, bottom panel (for $t = t2$), the probes indent the inhibitory region of the STRF, resulting in a net decrease in the predicted response, which is in agreement with the zero response at $t = t2$. In this manner, the predicted response is computed (Fig. 1*B*, center panel, black) and shown together with the observed number of spikes (Fig. 1*B*, center panel, magenta) during each 10 ms time window. We found a general agreement between the observed response and the firing rate predicted by the STRF, although the STRF predictions typically underestimate the observed response particularly at high firing rates (Fig. 1*B*) (correlation coefficient between the STRF prediction and observed response, 0.45) (see also Fig. 9). The STRF in Figure 1 also illustrates several characteristics exhibited by all STRFs. First, excitation generally occurs at shorter time lags relative to inhibition. Second, excitatory and inhibitory regions at short lags are replaced by a larger inhibitory region at the same location. Finally, the STRF is mostly restricted to within ~80 ms. In other words, the neural response at a given time is a function of the stimulus delivered in the preceding 80 ms.

Typical STRFs of peripheral afferents and cortical neurons are shown in Figure 2. In these and subsequent figures, the STRF is displayed as a standard spatiotemporal kernel (i.e., time axis of the STRF is reversed relative to the STRF in Fig. 1*B*). It must be emphasized that the STRF describes the spatial contributions of the stimulus at different delays preceding a spike. Because these neurons are driven by indentation amplitude (Johnson, 2001), stimuli shortly before a spike will be weighted positively, resulting in excitation in the STRF at short time lags. Similarly, because refractoriness in the neural response inhibits spike production (Dayan and Abbott, 2001), the occurrence of a spike at time t is inhibited by stimuli that cause spikes shortly before this time. As a result, stimuli at longer time lags are generally weighted negatively, resulting in inhibition in the STRF.

Surround and replacing inhibition

Given the lack of evidence for synaptic interactions in the periphery, inhibition in peripheral afferents may arise through two mechanisms. The first mechanism is the instantaneous skin mechanical suppression of the response when multiple probes indent the receptive field (Vega-Bermudez and Johnson, 1999b). The second mechanism is the suppression of a response for a short period after a spike (Dayan and Abbott, 2001). Because these mechanisms act at different times, the inhibition in the STRF caused by them can be distinguished by examining the temporal relationship of inhibition relative to excitation. To that end, inhibitory pixels that appeared simultaneously with excitation (but not after the excitatory peak) were classified as surround inhibition, whereas inhibitory pixels that followed the excitatory peak were classified as replacing inhibition. Thus, the STRFs in Figures 1*B* and 2*A* exhibit surround and replacing inhibition, whereas the RA afferent STRF in Figure 2*B* exhibits only replacing inhibition.

STRFs of peripheral afferents

STRFs from typical SA1 and RA afferents are illustrated in Figure 2, *A* and *B*. SA1 afferent STRFs exhibited a small, localized excitatory region with a weak surround inhibitory region that lasted ~15 ms, followed by replacing inhibition lasting nearly 30 ms (Fig. 2*A*). In contrast, RA afferent STRFs exhibited a somewhat larger excitatory region with no surround inhibition, which lasted ~15 ms, followed by replacing inhibition lasting ~30 ms (Fig. 2*B*). The total duration of the STRFs of these afferents is ~40–60 ms. The nonzero excitation in the first STRF slice is attributable to residual temporal autocorrelation effects in the STRF (see Materials and Methods).

STRFs from cortical areas 3b and 1

Cortical STRFs typically consisted of an initial excitatory region (sometimes with a flanking region of surround inhibition) appearing at ~15 ms, followed by a long period of replacing inhibition. As in previous studies of cortical receptive fields (DiCarlo and Johnson, 2002), we found a considerable variety in the STRFs of cortical neurons in areas 3b and 1. These STRFs could broadly be grouped into three types, depending on the temporal and

spatial arrangement of the inhibitory region(s) relative to the excitatory region. Examples of these three types of STRFs are shown in Figure 2*C–E*. The first type consisted of neurons with little or no inhibition (i.e., with an inhibitory volume that was <10% of the total excitatory volume) (Fig. 2*C*) (volume is defined as the sum of positive or negative weights across all probes and delays). The second type consisted of neurons with little or no surround inhibition but having replacing inhibition (Fig. 2*D*). We classified a neuron as belonging to this type if the surround inhibitory volume was <20% of the excitatory volume and comprised <50% of the total inhibitory volume. The third type consisted of neurons with substantial surround as well as replacing inhibition (surround inhibitory volume >50% of the total inhibitory volume or surround volume >20% of the excitatory volume) (Fig. 2*E*). We did not observe neurons with purely surround inhibition but no replacing inhibition. The proportions of the three types of neurons were as follows: 6% (2 of 33), 42% (11 of 33), and 52% (17 of 33) in area 3b, and 11% (5 of 44), 25% (11 of 44), and 64% (28 of 44) in area 1. Thus, area 1 has more cells with surround inhibition and fewer cells with purely replacing inhibition compared with area 3b. Similar proportions were found using protocol B. Although the spatial arrangements of the excitatory and surround inhibitory regions were similar to those described by DiCarlo et al. (1998), only about one-half of the cortical neurons exhibited surround inhibition.

STRF characteristics

In this section, we characterize the relative spatial positions, shapes, and relative timing of the excitatory and inhibitory STRF subregions of peripheral afferents and cortical neurons.

STRF area

The STRF area is a measure of the region on the skin that contributes to the neural response, and approximates the size of the classical receptive field on the distal fingerpad. We measured the STRF area as the total area occupied by nonzero pixels across all slices. Figure 3*A* illustrates a cumulative histogram of the total area on the distal fingerpad occupied by the STRFs of peripheral and cortical neurons. All STRF areas were enclosed within the stimulator area (stimulator area, 100 mm^2; largest STRF area, 61 mm^2). In the periphery, SA1 afferents had smaller STRF areas compared with RA afferents (mean areas, SA1, 18.7 mm^2; RA, 25 mm^2; $p < 0.05$, *t* test) (Fig. 3*A*). Nearly 80% of all cortical neurons had STRF areas larger than the mean SA1 afferent STRF area. In contrast, 60% of all cortical neurons had STRF areas that exceeded the average RA afferent STRF area. The STRF areas of area 3b and area 1 neurons were statistically identical (*t* test, $p > 0.1$; mean areas, area 3b, 30.3 mm^2; area 1, 26.8 mm^2) (Fig. 3*A*). Receptive field sizes for area 3b neurons are almost identical to those reported by DiCarlo et al. (1998).

Excitatory and inhibitory areas

Compared with SA1 afferents, RA afferents had significantly larger excitatory areas (RA, 22.3 mm^2; SA1, 11.3 mm^2; $p < 0.05$, *t* test) (Fig. 3*B*), and smaller inhibitory areas (RA, 12.8 mm^2; SA1, 16.7 mm^2; $p < 0.05$, *t* test) (Fig. 3*B*). The area devoted to surround suppression was more than twice as large in SA1 compared with RA afferents (RA, 2.8 mm^2; SA1, 7.2 mm^2; $p < 0.05$, *t* test) (data not shown). In cortex, excitatory regions of areas 3b and 1 were similar in size (area 3b, 19.7 mm^2; area 1, 18.2 mm^2; $p > 0.1$, *t* test) (Fig. 3*B*), whereas inhibitory regions were significantly larger in area 3b (*t* test, $p < 0.05$; area 3b, 22.8 mm^2; area 1, 17.3 mm^2) (Fig. 3*B*).

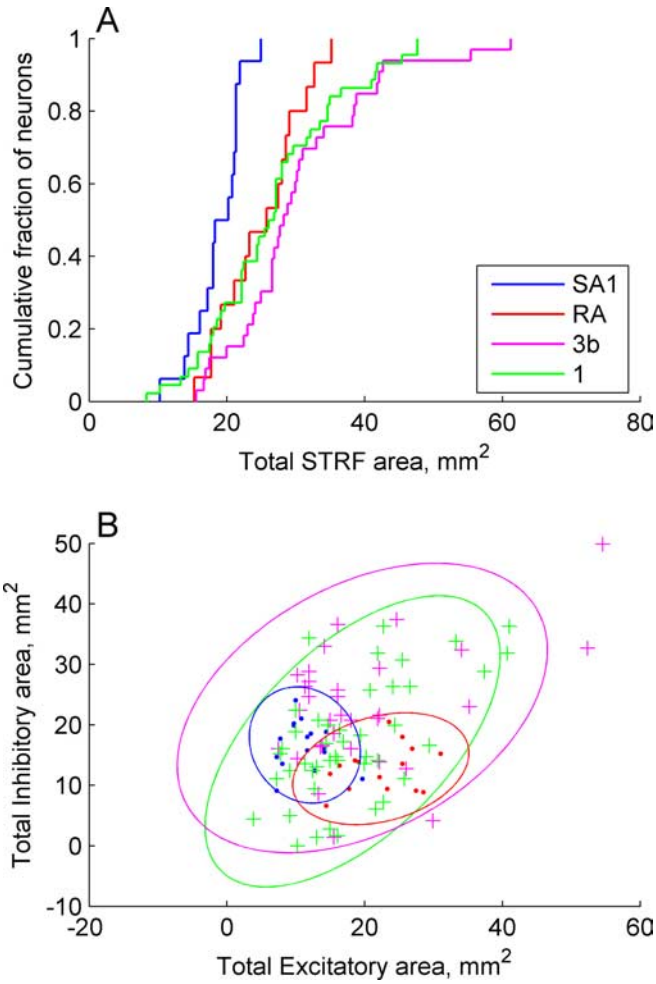

Figure 3. Peripheral and cortical STRF areas. ***A***, Cumulative histogram of the total area occupied by the STRF on the distal fingerpad (total probe area, 100 mm^2). Total area is calculated as the area occupied by all STRF pixels significantly different from zero. ***B***, Relationship between inhibitory and excitatory areas. Blue dots, peripheral SA1; red dots, peripheral RA; magenta crosses, cortical area 3b; green crosses, cortical area 1. Ellipses of the corresponding color indicate the area enclosed by 95% of the data, assuming a Gaussian distribution with the observed mean and covariance.

Temporal evolution of STRF areas

Figure 4 illustrates the time course of the evolution of the peripheral and cortical STRF areas. In the periphery, the STRF appears rapidly within the first 5 ms and decays rapidly over the next 10 ms, after which its size declines gradually (Fig. 4*A*). In Figure 4*B*, the evolution of excitatory and inhibitory areas of the STRF are shown separately. From this figure, it can be seen that, in SA1 afferents, the initial rapid response is composed of an excitatory component along with a smaller rapid inhibitory component. In contrast, RA afferents are dominated by excitation at short lags. At ~15 ms, these fast components of the receptive field are replaced by inhibition that decays slowly.

The time courses of cortical STRFs differ considerably from their peripheral afferent counterparts; the total area attains a peak ~10 ms later, which is expected because these neurons receive afferent input (peak locations: area 3b, 12 ms; area 1, 18 ms) (Fig. 4*A*). Figure 4*C* indicates the evolution of the excitatory and inhibitory areas over time. As in the periphery, both area 3b and area 1 neurons exhibit an initial phase of excitation and surround inhibition that is then replaced entirely by an inhibitory region. In contrast to the separation observed in the peripheral afferent

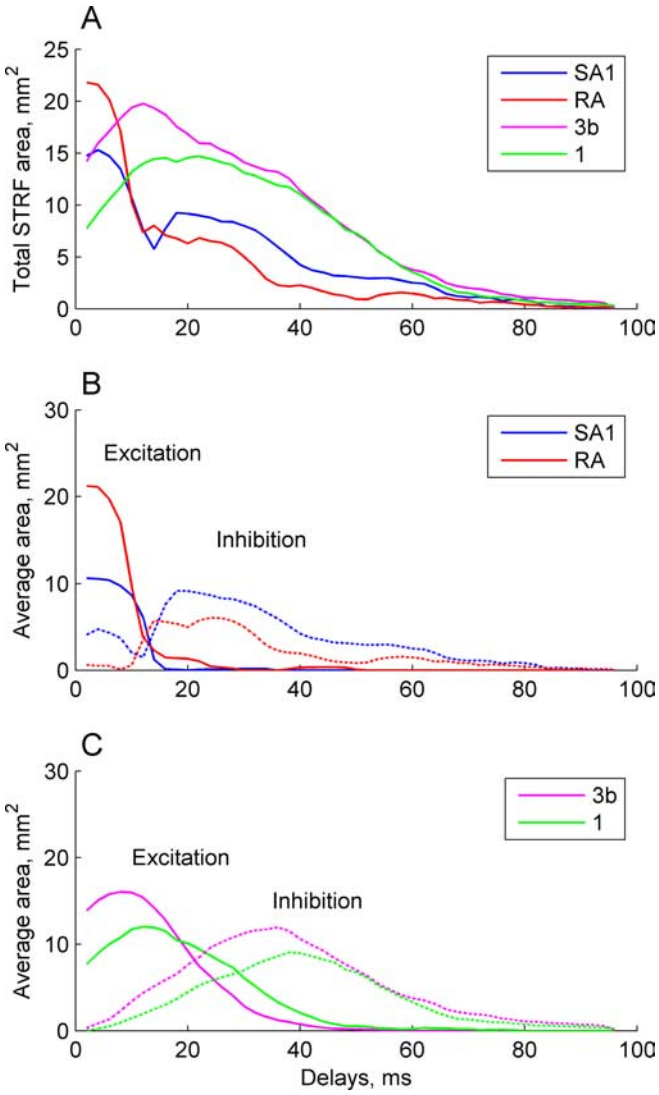

Figure 4. Temporal evolution of STRF areas. ***A***, Total (excitatory plus inhibitory) STRF area as a function of time, averaged over all neurons of a given afferent type or cortical area. ***B***, Average areas of excitatory (solid lines) and inhibitory (dotted lines) regions over time for peripheral SA1 and RA afferents. ***C***, Average areas of excitatory (solid lines) and inhibitory (dotted lines) regions over time for cortical areas 3b (magenta) and 1 (green).

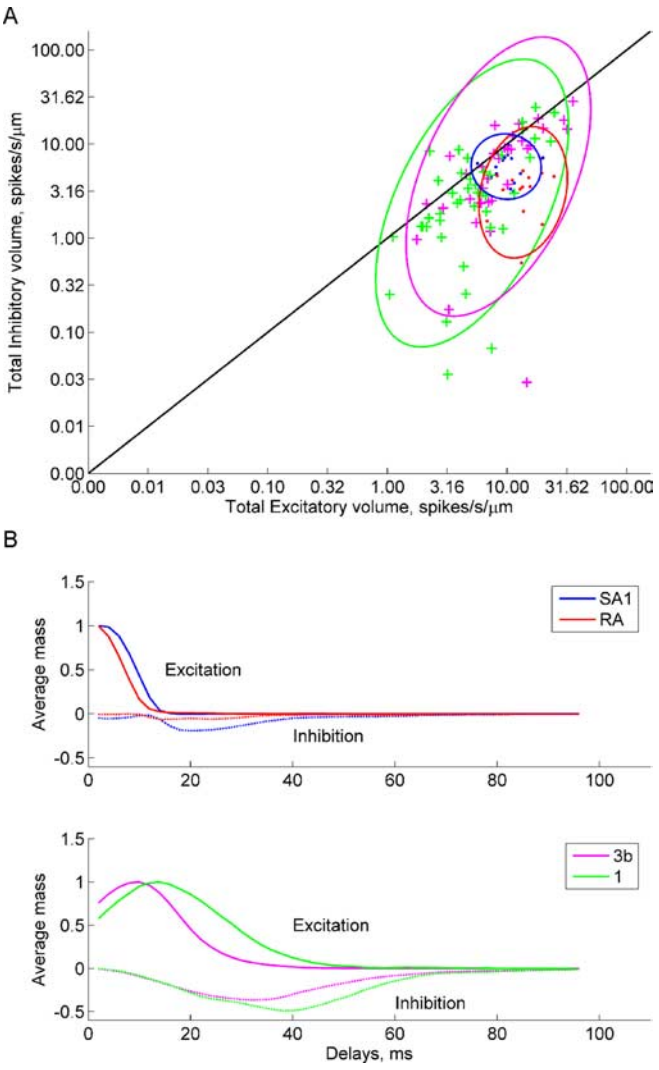

Figure 5. Peripheral and cortical STRF volumes. ***A***, Inhibitory versus excitatory volumes (i.e., mass summed over all delays), in logarithmic scale. For a description of the symbols, see Figure 3. ***B***, Average excitatory (solid lines) and inhibitory (dotted lines) mass as a function of time for peripheral afferents (top panel) and in areas 3b and 1 (bottom panel).

STRFs, inhibition in cortical STRFs could not be easily separated into surround and replacing inhibitory components based on the time course alone. Although the responses in area 1 evolve slightly later than area 3b responses (peak locations: area 3b, 12 ms; area 1, 18 ms), the total duration is ~70 ms for neurons in both areas.

STRF volume

Each region on the skin contacted by a probe may have a large or small effect on the firing rate depending on the magnitude of the corresponding weight in the STRF. To summarize this aspect of the response, we defined the total excitatory (inhibitory) volume as the net positive (negative) weight in the STRF, summed over all probes and delays. Thus, the excitatory (inhibitory) volume represents the average increase in firing rate that is caused by a 1 μm indentation in the excitatory (inhibitory) region in the STRF, and is specified in units of spikes per second per micrometer. We use the term "mass" (instead of volume) to denote the sum of STRF weights at a single delay rather than across delays (Fig. 5*B*).

A plot of total inhibitory volume versus total excitatory volume is shown in Figure 5*A*. In the periphery, RA afferent STRFs had larger excitatory volumes compared with SA1 STRFs (mean excitatory volumes, SA1, 10.2 spikes $\cdot$ s^{-1} $\cdot$ μm^{-1}; RA, 14.4 spikes $\cdot$ s^{-1} $\cdot$ μm^{-1}; *t* test, $p < 0.05$), as well as smaller inhibitory volumes (SA1, 6 spikes $\cdot$ s^{-1} $\cdot$ μm^{-1}; RA, 3.6 spikes $\cdot$ s^{-1} $\cdot$ μm^{-1}). Consequently, SA1 afferents also had a much larger ratio of inhibition to excitation compared with RAs (see below, Ratio of inhibition to excitation). Excitatory and inhibitory volumes in cortex were similar to those observed in the periphery. The average excitatory volume in cortex was slightly larger in area 3b compared with area 1 (area 3b, 10.8 spikes $\cdot$ s^{-1} $\cdot$ μm^{-1}; area 1, 6.7 spikes $\cdot$ s^{-1} $\cdot$ μm^{-1}; $p < 0.1$, *t* test). Inhibitory volume was also considerably larger in area 3b compared with area 1 (area 3b, 7.8 spikes $\cdot$ s^{-1} $\cdot$ μm^{-1}; area 1, 4.7 spikes $\cdot$ s^{-1} $\cdot$ μm^{-1}; *t* test, $p < 0.05$). However, the volume taken up by surround inhibition was statistically identical in the two areas (area 3b, 2.95 spikes $\cdot$ s^{-1} $\cdot$ μm^{-1}; area 1, 2.5 spikes $\cdot$ s^{-1} $\cdot$ μm^{-1}; *t* test, $p > 0.5$). Therefore, the difference in inhibitory volume between the two areas arises solely from differences in the strength of replac-

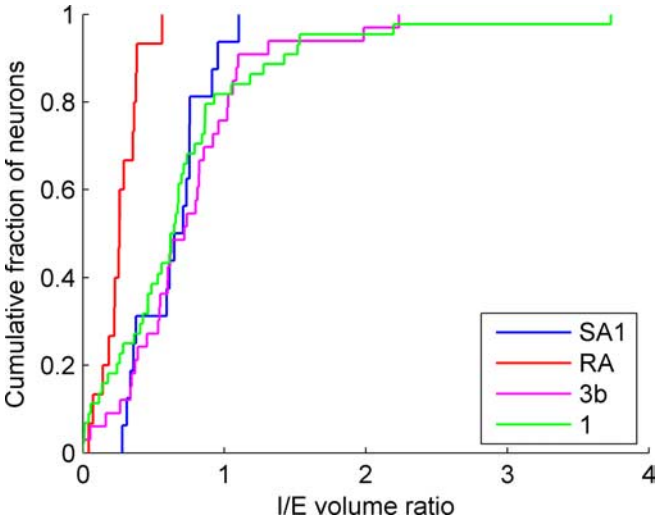

Figure 6. Ratio of inhibitory to excitatory volume. *I/E* ratio is computed as the ratio between total inhibitory volume to the total excitatory volume. For a description of the symbols, see Figure 3.

ing inhibition (see below, Properties of replacing and surround inhibition) (see Fig. 7).

Temporal evolution of STRF volume

Figure 5*B* illustrates the temporal evolution of excitatory and inhibitory volume, averaged over all neurons from a given anatomical location or afferent type. In both periphery and cortex, inhibition typically appears slightly later relative to excitation. In the periphery, there is relatively little surround inhibition present simultaneously with excitation, particularly for RAs compared with SA1 afferents. We attribute this surround inhibition in the STRFs of SA1 afferents to skin mechanical effects (see Discussion). Figure 5*B* shows that the replacing inhibition disappears by ~35 ms when volume is considered rather than area (Fig. 4*B*). This replacing inhibition is most likely attributable to the relative refractoriness after an action potential (see Discussion). In cortex, the effect of surround inhibition during the initial phase of the response is considerably larger relative to the periphery. Surround and replacing inhibition are larger and more persistent in cortex than in the periphery, suggesting that they are partly attributable to additional cortical or subcortical interactions (see Discussion).

Ratio of inhibition to excitation

The distribution of the overall weights assigned to STRF pixels determines the contribution of STRF regions to the neural response, and the overall balance between inhibition and excitation. We measured the ratio of total inhibitory volume to the total excitatory volume (*I*/*E* ratio); this is shown in Figure 6. The *I*/*E* ratio was always smaller than unity in all peripheral afferent STRFs, and was larger in SA1 compared with RA afferents (mean ratios: SA1, 0.64; RA, 0.27; *t* test, $p < 0.05$). The *I*/*E* ratio in cortex was comparable with the ratios observed in SA1 afferents but was considerably larger compared with RA afferents and did not differ between areas 3b and 1 (mean ratios: area 3b, 0.75; area 1, 0.71; *t* test, $p > 0.5$).

Properties of replacing and surround inhibition

We characterized the relative contributions of replacing and surround inhibition by measuring the fraction of total inhibitory volume that constituted replacing inhibition, as well as the temporal duration of surround and replacing inhibitory components (Fig. 7).

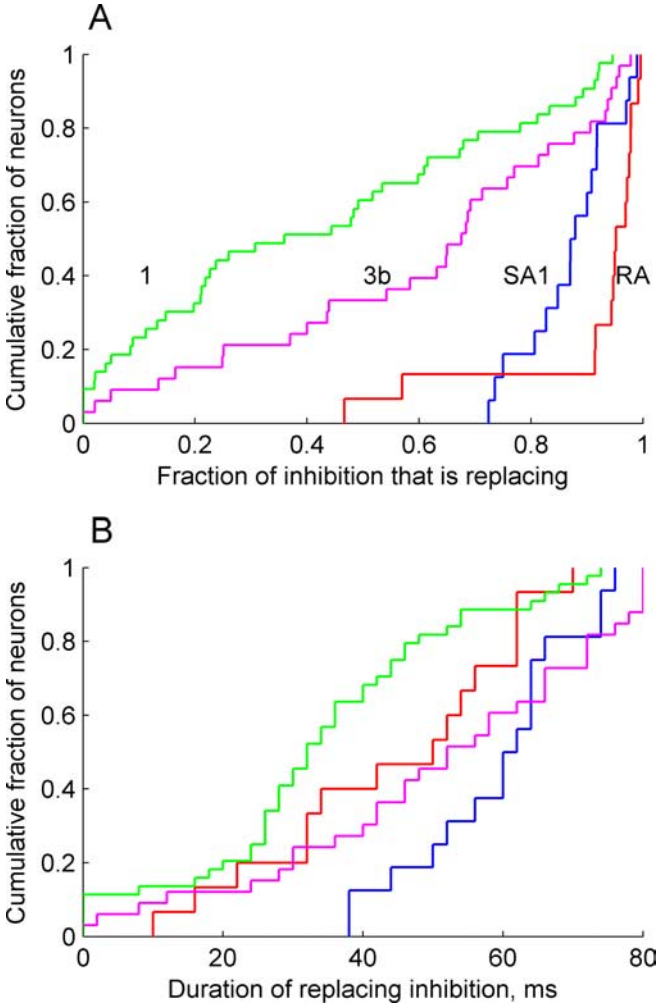

Figure 7. Properties of replacing inhibition. ***A***, Cumulative histogram of the proportion of inhibitory volume that constituted replacing inhibition in each STRF. ***B***, Cumulative histogram of the temporal duration of replacing inhibition. For a description of the symbols, see Figure 3.

In the periphery, surround inhibition constituted ~13% of the total inhibitory volume in SA1 afferents and 10% in RA afferents. Surround inhibition also constituted 42% of the total inhibitory area in SA1 and 23% in RA afferent STRFs. Surround inhibition lasted 30 ms in SA1 but only 12 ms in RA STRFs. Replacing inhibition lasted longer in SA1 than in RA STRFs (mean duration: SA1, 59 ms; RA, 44 ms; *t* test, $p < 0.05$). In cortex, there were considerable differences in replacing inhibition between areas 3b and 1. Replacing inhibition accounted for a higher proportion of the inhibition in area 3b compared with area 1 (area 3b, 60%; area 1, 41%; *t* test, $p < 0.05$) (Fig. 7*A*). Furthermore, replacing inhibition lasted longer in area 3b compared with area 1 (area 3b, 50 ms; area 1, 27 ms; *t* test, $p < 0.05$) (Fig. 7*B*). Contributions of surround and replacing inhibition to the inhibitory area were identical between the two areas (data not shown).

Temporal evolution of STRF shape

Neuronal responses in primary sensory areas are dominated by linear mechanisms (Jones and Palmer, 1987a; Palmer et al., 1991; DiCarlo et al., 1998; Ringach, 2004). As a result, properties such as direction, shape, or orientation selectivity arise primarily as a result of the shape, size, and orientation of the excitatory and

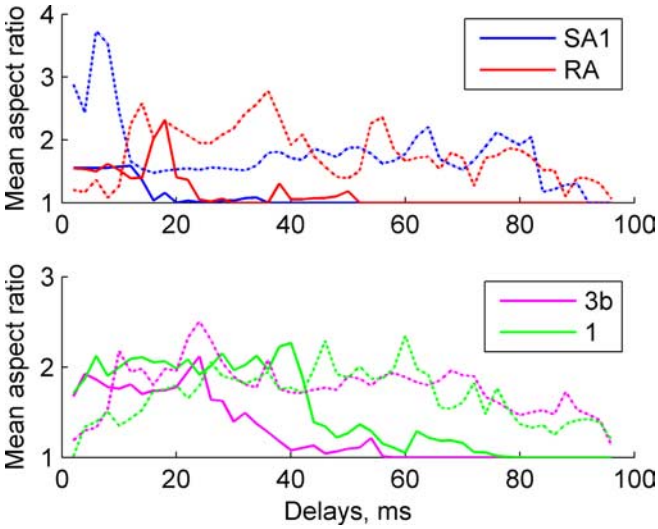

Figure 8. Temporal evolution of excitatory and inhibitory lobe aspect ratios. Average aspect ratios were computed at each time slice for excitatory (solid lines) and inhibitory regions (dotted lines), for peripheral afferents (top panel) and for cortical areas 3b and 1 (bottom panel). For a description of the symbols, see Figure 3.

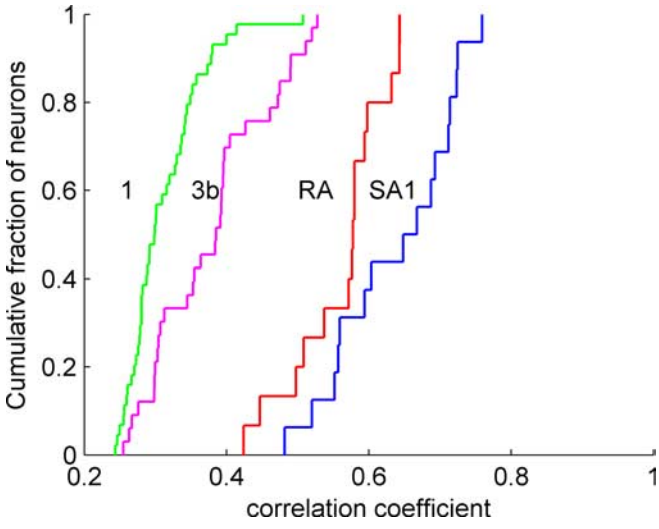

Figure 9. Peripheral and cortical STRF performance. STRF performance is measured as the correlation coefficient between the STRF model prediction and the observed response. For a description of the symbols, see Figure 3.

inhibitory regions in the receptive field (Jones and Palmer, 1987b; DiCarlo et al., 1998; Ringach, 2004). To examine these properties and how they are modulated over time, we fitted the excitatory and inhibitory regions of each STRF slice to two-dimensional Gaussian ellipsoids. The parameters of this fit are the major and minor axes, and the orientation of the ellipsoid. The aspect ratio (i.e., ratio of the major axis to the minor axis) is a measure of the ellipticity of the region, where a unit aspect ratio indicates a circular region.

We computed the average aspect ratio (over all STRF slices) for peripheral and cortical STRFs. The average aspect ratios were similar in both periphery and cortex (average aspect ratios: excitatory lobe, SA1, 1.55; RA, 1.6; inhibitory lobe, SA1, 1.5; RA, 1.9). Interestingly, although the size of receptive fields in cortex may be larger than their peripheral afferent counterparts, the aspect ratios in cortex were similar to those observed in the periphery (excitatory lobe, area 3b, 1.6; area 1, 2.0; inhibitory lobe, area 3b, 2.0; area 1, 2.2). The temporal evolution of the aspect ratio of excitatory and inhibitory regions in the STRFs is shown in Figure 8. We found that the aspect ratio of the excitatory region in both peripheral and cortical neurons remains relatively constant over the initial part of the response. In contrast, the inhibitory region undergoes a gradual evolution over time, from an increasingly elongated shape that then becomes more circular with time; this is because the early STRF slices are dominated by surround inhibition, which is often elongated (Figs. 1, 2*E*). Subsequent STRF slices are dominated by replacing inhibition, which is more circular in shape. Note that these trends are more noticeable in periphery compared with cortex; this is consistent with the larger variety in receptive field shapes observed in cortex. Finally, 50% of peripheral afferents had nearly circular peak excitatory regions (i.e., aspect ratios <1.5), whereas in cortex, only 35% of the STRFs had circular excitatory regions.

We did not observe any changes in the orientation of the excitatory and inhibitory regions over time. In the periphery, excitatory lobe orientations had considerable variance, although they tended to be oriented along the long (i.e., distal–proximal) axis of the finger (circular mean orientations: SA1, 111°; RA, 91° counterclockwise from horizontal). Inhibitory lobe properties were very similar (aspect ratios: SA1, 1.5; RA, 2.0; circular mean orientations: SA1, 95°; RA, 91°), although there is greater variation in the lobe orientation. In cortex, the orientation of excitatory regions was similar to the orientations observed in periphery. Furthermore, the orientation of excitatory and inhibitory lobes was similar in areas 3b and 1, although inhibitory regions exhibited greater variation in orientation (circular mean orientations: peak excitatory region, area 3b, 97°; area 1, 80°; peak inhibitory region, area 3b, 104°; area 1, 87°) (data not shown).

Model goodness-of-fit

We measured the performance of the STRFs by computing the correlation coefficient between the STRF prediction and the observed response. A low correlation coefficient indicates that the (linear) STRF model is unable to account for the response modulations (see Discussion). In the periphery, we found that STRFs of SA1 afferents were able to predict their responses to the STRI stimuli significantly better than RAs (mean correlations: SA1, 0.64; RA, 0.56; *t* test, $p < 0.05$) (Fig. 9). In cortex, STRFs of area 3b performed better compared with area 1 STRFs (mean correlations: area 3b, 0.38; area 1, 0.31; *t* test, $p < 0.05$) (Fig. 9).

Space–time separability of STRFs

Spatiotemporal receptive fields estimated in visual cortex have been examined for space–time separability (Cai et al., 1997), which indicates whether the receptive field can be decomposed into the product of a spatial kernel with a temporal kernel. If an STRF consisted of excitation alone, then it can clearly be decomposed into a spatial kernel (excitatory region) multiplied by a temporal kernel (i.e., an exponential decay). Similarly an STRF with excitation and replacing inhibition is the product of a spatial kernel (the excitatory region) multiplied by a temporal kernel (i.e., a difference of two exponential decays). Thus, STRFs of the first two types (i.e., with excitation only or with excitation followed by replacing inhibition) are space–time separable. In contrast, STRFs of the third type (i.e., with both surround and replacing inhibition) cannot be characterized as the product of a spatial kernel with a temporal kernel. A majority of the STRFs in cortex (52% in area 3b; 64% in area 1) consisted of both surround and replacing inhibition, and were therefore space–time insepa-

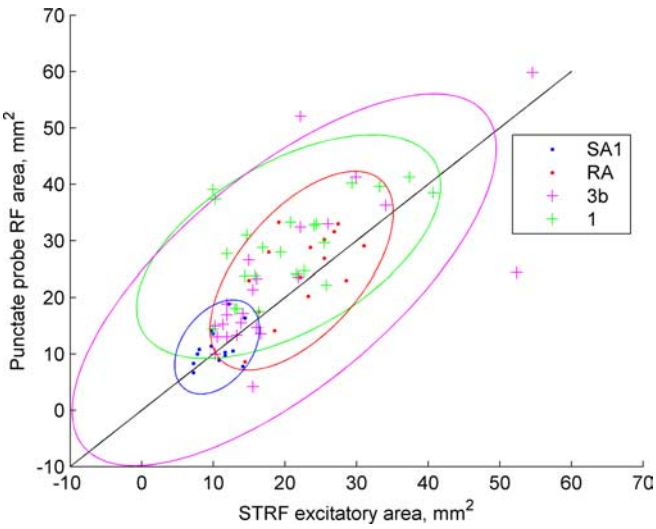

Figure 10. Comparison of STRF area with punctate probe receptive field areas. Punctate probe RF area plotted against STRF total area. Data are shown for SA1 afferents (blue dots), RA afferents (red dots), area 3b neurons (magenta crosses), and area 1 neurons (green crosses). Ellipses of the corresponding color indicate the area enclosed by 95% of the data, assuming a Gaussian distribution with the observed mean and covariance.

rable. In contrast, peripheral RA (but not SA1) afferent STRFs were space–time separable.

Relationship between STRF and punctate probe receptive fields

Several studies have examined cortical and peripheral neuronal responses using punctate probes. For a subset of the neurons (periphery: SA1, 16; RA, 15; cortex, area 3b, 24; area 1, 23), we compared the STRF with the response map obtained by indenting individual probes of the 400-probe array into the skin by 300 μm at each location (Fig. 10) (see Materials and Methods). The STRF model predicts that inhibitory regions affect the response only if they are simultaneously activated along with an excitatory region. Thus, a punctate probe stimulus is predicted to evoke responses from the excitatory regions alone. The average response evoked by the punctate probe indentation at each location in the array is referred to as the punctate probe RF. We found that the responses predicted by the STRF to punctate probes agreed well with the observed punctate probe RF, in both periphery and cortex (mean correlations: SA1, 0.93; RA, 0.88; area 3b, 0.69; area 1, 0.60).

Periphery. The total STRF area exceeded the punctate probe RF area in all SA1 afferents and in about one-half of the RA afferents. We suggest that this difference is attributable to the contribution of the surround inhibition observed in peripheral STRFs. We also found that, as expected, RA afferents had larger punctate probe RF areas compared with SA1 afferents. We observed a high correlation between punctate probe RF area and STRF excitatory area and a somewhat weaker correlation with STRF total area (correlations: 0.84 and 0.50, respectively) (Fig. 10). We also computed the relative location of the centers of mass of excitatory and inhibitory regions of the STRF relative to the center of mass of the punctate probe RF. Locations of the excitatory centers were in close agreement (correlation, 0.89), whereas the locations of the STRF inhibitory centers are loosely correlated with the punctate probe receptive field center (correlation, 0.4) (data not shown).

Cortex. The total STRF area exceeded the punctate probe RF area in ~79% (19 of 24) neurons in area 3b, and in 65% (15 of 23) neurons in area 1 (data not shown). As in the periphery, we observed a high correlation between punctate probe RF area and STRF excitatory area, and a lower correlation with STRF total area (correlations: 0.64 and 0.46, respectively) (see Discussion). The location of the center of mass of the punctate probe receptive field was in close agreement with the STRF excitatory center of mass (correlation, 0.85) and was loosely correlated with the inhibitory center of mass (correlation, 0.34).

Overall, the data from both peripheral and cortical neurons indicate that the punctate probe RF is closely related to the excitatory region of the STRF and that the STRFs are a reasonable characterization of the neural response.

Response properties

For each neuron, we measured the mean, variability, and latency of the responses evoked by the STRI stimulus. Some of these properties are indirectly related to the STRF; for example, the measured STRF volume is high when the evoked firing rate is high, and the latency is related to the temporal evolution of STRF excitatory and inhibitory regions. In a subsequent experiment (protocol B), we also examined the effect of indentation density on the response.

Response latency

Here, we describe an alternate method to estimate the response latency. Because each probe movement lasted 20 ms, the STRF cannot be used to obtain precise estimates of the response latency. Therefore, for each probe, we obtained the average neural response after each indentation. The resulting "indentation-triggered response" for each probe is the average change in the neural response attributable to the onset of a given indentation. Thus, for a probe outside the receptive field, the indentation-triggered response will be flat. For a probe in the receptive field of the neuron, the response curve will deviate above or below the average level depending on whether the region is excitatory or inhibitory. We defined the peak response latency as the time of the maximum indentation-triggered response of the probes in the excitatory region of the STRF. It must be emphasized that, although the response curve shares many characteristics of the STRF, it is not an estimate of the underlying linear transfer function of the neuron. In the periphery, RAs had somewhat shorter peak latencies compared with SA1s (mean latencies for upper arm recordings: SA1, 14.0 ms; RA, 13.2 ms; lower arm recordings, SA1, 13.5 ms; RA, 10.4 ms). When separated by afferent type and recording location, samples were too few to perform statistical tests or to obtain reliable estimates of the conduction velocity. In cortex, area 3b neurons had significantly shorter peak latencies compared with area 1 neurons (mean latencies: area 3b, 26.4 ms; area 1, 31.1 ms; $p < 0.05$, t test). However, latency differences between area 3b and 1 were not significant in the other monkey (protocol B; mean latencies, area 3b, 22.1 ms; area 1, 23.2 ms; $p > 0.05$, t test). Therefore, we concluded that the response latencies are comparable in areas 3b and 1.

Mean and variability of responses evoked to STRI stimuli

We observed a gradual decrease in responsiveness to the STRI stimuli from periphery to cortex. In the periphery, RAs responded more vigorously to the STRI stimulus compared with the SA1s (average firing rates, SA1, 35.7 spikes/s; RA, 76.9 spikes/s; t test, $p < 0.05$). In cortex, area 3b neurons responded more vigorously to random indentations (average firing rates: area 3b, 25.7 spikes/s; area 1, 19.8 spikes/s; t test, $p < 0.05$). This progressive decrease in responsiveness from periphery to area 3b to area 1 and the concomitant decrease in response linearity (Fig.

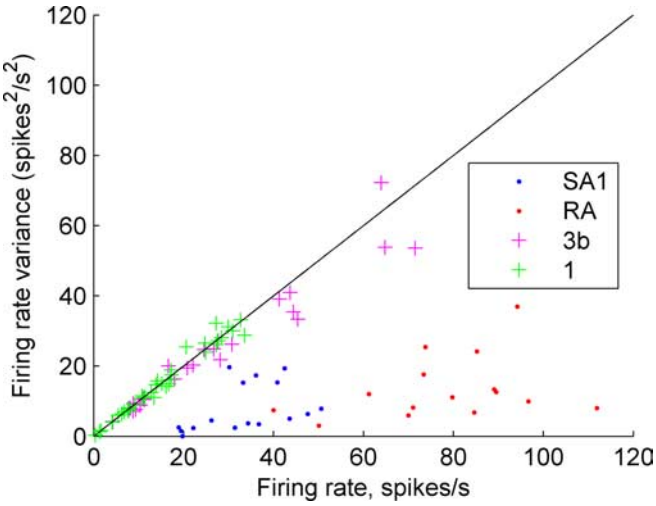

Figure 11. Response mean and variability. Firing rate variance versus mean firing rate plotted for peripheral and cortical responses to the STRI stimulus. Firing rate mean and variance were computed over three repeats for each 10 ms bin, and then averaged over the entire 200 s of the response. Data are from protocol B (see Materials and Methods). The solid black line indicates the unity line. Blue dots, SA1 afferents; red dots, RA afferents; magenta crosses, area 3b neurons; green crosses, area 1 neurons.

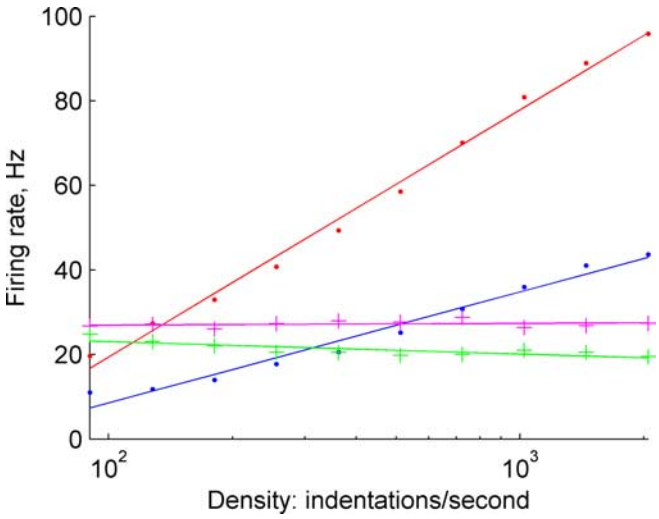

Figure 12. Effect of indentation density on peripheral and cortical firing rates. Population average firing rates of SA1 (blue; dots) and RA (red; dots) afferents, and those of area 3b (magenta; crosses) and area 1 (green; crosses), are shown as a function of the stimulus indentation density (shown in logarithmic scale). Data are from protocol B.

9) indicate the emergence of selectivity in the response to complex features that are most likely absent in the STRI stimulus. In protocol B, we measured the response variability by plotting the firing rate variance versus its mean (Fig. 11). As expected, peripheral responses were more repeatable (slopes: SA1, 0.29; RA, 0.15), whereas cortical responses exhibited high discharge variability comparable with that of a Poisson discharge (slopes: area 3b, 0.86; area 1, 1.0).

Effect of indentation density

In protocol B, short segments of the STRI stimulus with different indentation densities were run to examine the effect on the firing rate, and to determine the preferred indentation density for STRF estimation. Figure 12 shows the mean firing rate, computed across over each type of neuron (i.e., over peripheral SA1, peripheral RA, area 3b and area 1 neurons). Both SA1 and RA afferents exhibited firing rates that were proportional to the logarithm of indentation density (i.e., firing rate $r = a.\log_{10}(\text{density}) + b$; SA1, $a = 26.3$, $b = -44.0$; RA, $a = 58.5$, $b = -97.55$). In contrast, the firing rates of both area 3b and area 1 neurons were unaffected by the indentation density (area 3b, $a = 0.39$, $b = 26.2$; area 1, $a = -2.9$, $b = 28.9$). Peripheral afferent STRFs exhibited a decrease in overall area with indentation density, which is likely to be attributable to surround suppression. In contrast, cortical STRFs exhibited little or no variation in STRF characteristics with indentation density (data not shown).

STRFs obtained using different protocols

We recorded the responses of peripheral and cortical neurons to two STRI protocols (see Materials and Methods). There were two principal differences in protocol B compared with protocol A: (1) the probe movements had a larger indentation velocity and shorter duration to reduce stimulus temporal autocorrelation; (2) the total stimulus duration was made shorter to accommodate stimulus repetitions. These modifications did not affect most aspects of the data (e.g., firing rates, total STRF areas, etc.). Even the aspects of the data that were affected by the stimulus modifications were modulated uniformly across neurons, resulting in identical trends in the results from both protocols. There were three main differences in the data from the two protocols. (1) The larger indentation velocity in protocol B made it a slightly more effective stimulus. As a result, response latencies in the data were shorter by ~4 ms (periphery, lower arm: SA1, 9.2 ms; cortex, area 3b, 26.4 ms; area 1, 33.0 ms). (2) The shorter probe indentation waveform in protocol B led to better removal of temporal autocorrelation in the STRF. As a result, the extent to which the STRF model predicted the data were higher in protocol B compared with A (mean correlations, SA1, 0.64; RA, 0.53; area 3b, 0.54; area 1, 0.41). Excitatory and inhibitory regions had shorter temporal extents for the same reason. The temporal autocorrelation correction was identical for all of the data, allowing the comparison of results across neuron types and anatomical areas. (3) A shorter STRI stimulus duration meant that there was more noise in the STRF estimates. Because the inhibitory weights are generally smaller than excitatory weights, they are more susceptible to noise. As a result, inhibitory properties such as volume and area were generally smaller in the STRFs computed using protocol B.

Discussion

Previous studies in characterizing the neural representation of spatial form in the somatosensory pathway have taken two approaches. The first approach is to describe the population responses of peripheral and cortical neurons using identical stimuli (Phillips et al., 1988). The second approach is to characterize neural responses using models that predict responses to arbitrary stimuli (Bankman et al., 1990; DiCarlo et al., 1998). To that end, DiCarlo et al. (1998) estimated linear spatial receptive fields of area 3b neurons and then manipulated the stimulus scanning velocity to infer the temporal properties of excitation and inhibition (DiCarlo and Johnson, 2002). In this study, we elaborated on previous work in two ways: First, we directly estimated the spatiotemporal receptive field, describing the time course of excitation and inhibition. Second, we compared the properties of the STRFs across anatomical areas.

STRFs of peripheral SA1 and RA afferents

We observed considerable differences in the spatial properties of the STRFs of SA1 and RA afferents. RA afferents had larger exci-

tatory and total STRF areas compared with SA1 afferents, consistent with their lower spatial resolution (Johnson, 2001). Furthermore, SA1 afferents exhibit surround inhibition but RAs do not. We attribute this surround inhibition to skin mechanical effects for two reasons. First, there is no evidence for synaptic mechanisms in the periphery that could produce surround inhibition. Second, SA1 (but not RA) afferents exhibit enhanced edge responses to gratings (Phillips and Johnson, 1981) as well as surround suppression when multiple probes indent the receptive field (Vega-Bermudez and Johnson, 1999b). These skin mechanical effects result in a uniform suppressed response surrounding the excitatory region (Fig. 2*A*).

The time course of excitatory and inhibitory regions was slower in the STRFs of SA1 compared with RA afferents. A shorter time course for RAs is expected because they exhibit rapid response modulations. For example, the relative refractory period has been estimated to be 58 ms for SA1 and 29 ms for RA afferents (Freeman and Johnson, 1982), which corresponds well to the time courses reported here (Fig. 5). Therefore, replacing inhibition in both afferent types can be attributed to the relative refractoriness after a spike.

SA1 and RA afferents also differed in many response properties. First, RA afferents responded more vigorously to the STRI stimuli compared with SA1 afferents; this is not surprising given the dynamic nature of the stimulus and the higher velocity sensitivity of RA afferents (Johnson, 2001). Second, SA1 responses were more linear than RA responses. This difference in linearity is likely because of intrinsic differences between the afferent types. In particular, RA afferents respond to both the indentation and withdrawal of a stimulus, indicating their sensitivity to the magnitude (but not the sign) of stimulus velocity. This nonlinear velocity sensitivity in RAs cannot be accounted for by the linear STRFs.

STRFs of cortical neurons

Consistent with previous work (Hyvärinen and Poranen, 1978; Vierck et al., 1988; Iwamura et al., 1993), we found neurons frequently responsive to multiple fingerpads or multiple digits in area 1 but rarely so in area 3b. STRF areas measured on a single fingerpad, however, were similar in both areas 3b and 1, indicating that the organization of excitatory and inhibitory regions in these cortical areas is similar within fingerpads despite the difference in RF sizes.

Recent studies in area 3b (DiCarlo et al., 1998; DiCarlo and Johnson, 1999, 2000) have inferred that receptive fields consist of an excitatory and an inhibitory component that are fixed relative to each other, and a delayed inhibitory component. In this study, we directly estimated the relative timing of excitation and inhibition using the STRFs. The surround inhibition observed in the STRFs, being fixed relative to the excitatory region in its location (although it is slightly delayed), corresponds to the fixed inhibitory component. Similarly, the replacing inhibition in the STRF corresponds to the delayed inhibitory component (DiCarlo and Johnson, 2000).

The simplest explanation for the surround inhibition observed in cortex is that it arises directly from peripheral SA1 input. Three arguments lend support to the existence of additional underlying mechanisms: (1) the latency of the surround inhibitory component is ~10 ms after the appearance of excitation, implying the presence of additional synaptic connections; (2) the proportion of surround inhibition seen in cortex (>40%) far exceeds the proportion in the periphery (<13%) and is often asymmetrically located relative to the excitatory center; and (3) the ratio of surround inhibitory volume to excitatory volume in cortex is at least four times larger than the ratio in the periphery. There is also evidence from the visual cortex that surround inhibition is mediated by long-range lateral intracortical or feedback interactions (Weliky et al., 1995; Angelucci et al., 2002). Therefore, we suggest that surround inhibition observed in cortical STRFs is of intracortical origin.

The mechanisms underlying replacing inhibition in cortical STRFs are more difficult to explain. Although refractoriness must play a role, replacing inhibition plays an important role in the invariance to scanning velocity observed in area 3b responses (DiCarlo and Johnson, 1999). Furthermore, the differences in the properties of replacing inhibition in the two cortical areas (Fig. 7) suggest that replacing inhibition in cortex is not simply attributable to refractoriness but also attributable to active cortical interactions.

Functional differences between area 3b and area 1

We found that STRFs from area 3b and area 1 were similar in many aspects. Receptive fields in areas 3b and 1 had similar total areas (Fig. 3), similar durations (Fig. 4*A*,*C*), similar excitatory masses with similar time courses (Fig. 5*B*), similar inhibitory to excitatory ratios (Fig. 6), and similar aspect ratios. However, the STRFs differed considerably in other respects. STRFs of area 3b neurons had slightly larger inhibitory areas (Fig. 3*B*), more rapidly decaying excitatory and inhibitory volumes (Fig. 5*C*), and higher fraction and duration of replacing inhibition (Fig. 7). Finally, area 3b responses were predicted better by STRFs compared with area 1, suggesting that area 3b responses are more linear. These results suggest that area 3b and 1 neurons perform similar but not identical functions. Although the total excitatory masses are similar, the smaller degree of replacing inhibition in area 1 suggests a more complex spatial selectivity and less velocity sensitivity. Our results regarding the structure of receptive fields in areas 3b and 1 are mostly consistent with previous work. Surround inhibition has been reported in areas 3b and 1 in several studies (Pubols and LeRoy, 1977; Sur, 1980; DiCarlo et al., 1998; DiCarlo and Johnson, 1999, 2000). Direction and motion selectivity can also be attributed to receptive fields with surround inhibition (Warren et al., 1986; Murthy and Humphrey, 1999).

STRF goodness-of-fit

The agreement between STRF predictions and observed responses decreased gradually from periphery to area 3b to area 1, suggesting that an increasing proportion of the response deviates from the prediction of a linear model. Nevertheless, the estimated STRFs provide a first approximation to the neural response and, importantly, indicate the extent to which the response can be understood in terms of simple linear mechanisms. The relatively low correlations between STRF predictions and observed responses in this study are comparable with those reported in other cortical studies (DiCarlo et al., 1998; Theunissen et al., 2000; David et al., 2004). Although the STRFs may not predict responses to all stimuli, they do account for simpler response properties such as temporal and spatial frequency tuning (DeAngelis et al., 1993). A comparable result in this study is the accurate prediction of punctate probe responses by the STRFs.

Effect of indentation density

We found that afferent firing rates increased logarithmically with the indentation density (Fig. 12). Although the greater number of

probes reduces the overall response (Vega-Bermudez and Johnson, 1999b), the higher rate of indentation clearly dominated the peripheral afferent response, resulting in an increase in firing rate with indentation density.

In contrast to the periphery, cortical neurons had a nearly constant firing rate (Fig. 12) that did not change with indentation density. This behavior can be explained using a simple model: let the output firing rate r of a cortical neuron be proportional to the difference between excitatory (E) and inhibitory (I) contributions derived from peripheral afferents [$r = k(E - I)$]. Then, if E and I were proportional to the logarithm of the indentation density, the resultant firing rate would be invariant to indentation density. Thus, the invariance to indentation density can be attributed to the logarithmic dependence of peripheral afferent firing rates on indentation density, and to a difference operation in cortex.

Transformation of tactile information along the somatosensory pathway

The characteristics of the STRF provide important information about how tactile stimuli are represented in the periphery and cortex. Figures 4 and 5 illustrate the successive activation of excitation in peripheral RA and SA1 afferents, and then in area 3b and area 1 neurons. There is a gradual increase in the amount of surround inhibition from periphery to area 3b to area 1, suggesting increasingly complex spatial form processing along the processing hierarchy. Finally, area 1 responses are less linear, suggesting that it may be further along the pathway leading to an invariant tactile representation.

References

Aertsen AM, Johannesma PI (1981) The spectro-temporal receptive field. A functional characteristic of auditory neurons. Biol Cybern 42:133–143.

Angelucci A, Levitt JB, Walton EJ, Hupe JM, Bullier J, Lund JS (2002) Circuits for local and global signal integration in primary visual cortex. J Neurosci 22:8633–8646.

Bankman IN, Johnson KO, Hsiao SS (1990) Neural image transformation in the somatosensory system of the monkey: comparison of neurophysiological observations with responses in a neural network model. Cold Spring Harb Symp Quant Biol 55:611–620.

Cai D, DeAngelis GC, Freeman RD (1997) Spatiotemporal receptive field organization in the lateral geniculate nucleus of cats and kittens. J Neurophysiol 78:1045–1061.

Darian-Smith I, Goodwin AW, Sugitani M, Heywood J (1984) The tangible features of textured surfaces: their representation in the monkey's somatosensory cortex. In: Dynamic aspects of neocortical function (Edelman GM, Gall WE, Cowan WM, eds), pp 475–500. New York: Wiley.

David SV, Vinje WE, Gallant JL (2004) Natural stimulus statistics alter the receptive field structure of v1 neurons. J Neurosci 24:6991–7006.

Dayan P, Abbott LF (2001) Theoretical neuroscience: computational and mathematical modeling of neural systems. Cambridge, MA: MIT.

DeAngelis GC, Ohzawa I, Freeman RD (1993) Spatiotemporal organization of simple-cell receptive fields in the cat's striate cortex. II. Linearity of temporal and spatial summation. J Neurophysiol 69:1118–1135.

DeAngelis GC, Ohzawa I, Freeman RD (1995) Receptive-field dynamics in the central visual pathways. Trends Neurosci 18:451–458.

de Boer E, Kuyper P (1968) Triggered correlation. IEEE Trans Biomed Eng 15:169–179.

DiCarlo JJ, Johnson KO (1999) Velocity invariance of receptive field structure in somatosensory cortical area 3b of the alert monkey. J Neurosci 19:401–419.

DiCarlo JJ, Johnson KO (2000) Spatial and temporal structure of receptive fields in primate somatosensory area 3b: effects of stimulus scanning direction and orientation. J Neurosci 20:495–510.

DiCarlo JJ, Johnson KO (2002) Receptive field structure in cortical area 3b of the alert monkey. Behav Brain Res 135:167–178.

DiCarlo JJ, Lane JW, Hsiao SS, Johnson KO (1996) Marking microelectrode penetrations with fluorescent dyes. J Neurosci Methods 64:75–81.

DiCarlo JJ, Johnson KO, Hsiao SS (1998) Structure of receptive fields in area 3b of primary somatosensory cortex in the alert monkey. J Neurosci 18:2626–2645.

Freeman AW, Johnson KO (1982) A model accounting for effects of vibratory amplitude on responses of cutaneous mechanoreceptors in macaque monkey. J Physiol (Lond) 323:43–64.

Gardner EP (1988) Somatosensory cortical mechanisms of feature detection in tactile and kinesthetic discrimination. Can J Physiol Pharmacol 66:439–454.

Hsiao SS, Johnson KO, Twombly IA, DiCarlo JJ (1996) Form processing and attention effects in the somatosensory system. In: Somesthesis and the neurobiology of the somatosensory cortex (Franzén O, Johansson RS, Terenius L, eds), pp 229–247. Basel: Birkhäuser.

Hsiao SS, Lane JW, Fitzgerald P (2002) Representation of orientation in the somatosensory system. Behav Brain Res 135:93–103.

Hyvärinen J, Poranen A (1978) Movement-sensitive and direction and orientation-selective cutaneous receptive fields in the hand area of the post-central gyrus in monkeys. J Physiol (Lond) 283:523–537.

Iwamura Y, Tanaka M, Sakamoto M, Hikosaka O (1993) Rostrocaudal gradients in the neuronal receptive field complexity in the finger region of the alert monkey's postcentral gyrus. Exp Brain Res 92:360–368.

Johnson KO (2001) The roles and functions of cutaneous mechanoreceptors. Curr Opin Neurobiol 11:455–461.

Jones EG, Powell TPS (1970) Connexions of the somatic sensory cortex of the rhesus monkey. III. Thalamic connexions. Brain 93:37–56.

Jones JP, Palmer LA (1987a) The two-dimensional spatial structure of simple receptive fields in cat striate cortex. J Neurophysiol 58:1187–1211.

Jones JP, Palmer LA (1987b) An evaluation of the two-dimensional Gabor filter model of simple receptive fields in cat striate cortex. J Neurophysiol 58:1233–1258.

Lebedev MA, Nelson RJ (1996) High-frequency vibratory sensitive neurons in monkey primary somatosensory cortex: entrained and nonentrained responses to vibration during the performance of vibratory-cued hand movements. Exp Brain Res 111:313–325.

Merzenich MM, Kaas JH, Sur M, Lin CS (1978) Double representation of the body surface within cytoarchitectonic areas 3b and 1 in "SI" in the owl monkey (*Aotus trivirgatus*). J Comp Neurol 181:41–73.

Mountcastle VB, Powell TPS (1959) Neural mechanisms subserving cutaneous sensibility, with special reference to the role of afferent inhibition in sensory perception and discrimination. Bull Johns Hopkins Hosp 105:201–232.

Mountcastle VB, Reitboeck HJ, Poggio GF, Steinmetz MA (1991) Adaptation of the Reitboeck method of multiple microelectrode recording to the neocortex of the waking monkey. J Neurosci Methods 36:77–84.

Murthy A, Humphrey AL (1999) Inhibitory contributions to spatiotemporal receptive-field structure and direction selectivity in simple cells of cat area 17. J Neurophysiol 81:1212–1224.

Palmer LA, Davis TL (1981) Comparison of responses to moving and stationary stimuli in cat striate cortex. J Neurophysiol 46:277–295.

Palmer LA, Jones JP, Stepnoski A (1991) Striate receptive fields as linear filters: characterization in two dimensions of space. In: Vision and visual dysfunction. The neural basis of visual function (Leventhal AG, ed), pp 246–265. Boca Raton, FL: CRC.

Phillips JR, Johnson KO (1981) Tactile spatial resolution: II. Neural representation of bars, edges, and gratings in monkey primary afferents. J Neurophysiol 46:1192–1203.

Phillips JR, Johnson KO, Hsiao SS (1988) Spatial pattern representation and transformation in monkey somatosensory cortex. Proc Natl Acad Sci USA 85:1317–1321.

Prud'homme MJ, Cohen DA, Kalaska JF (1994) Tactile activity in primate primary somatosensory cortex during active arm movements: cytoarchitectonic distribution. J Neurophysiol 71:173–181.

Pubols LM, LeRoy RF (1977) Orientation detectors in the primary somatosensory neocortex of the raccoon. Brain Res 129:61–74.

Ringach DL (2004) Mapping receptive fields in primary visual cortex. J Physiol (Lond) 558:717–728.

Sur M (1980) Receptive fields of neurons in areas 3b and 1 of somatosensory cortex in monkeys. Brain Res 198:465–471.

Sur M, Merzenich MM, Kaas JH (1980) Magnification, receptive-field area,

and hypercolumn size in areas 3b and 1 of somatosensory cortex in owl monkeys. J Neurophysiol 44:295–311.

Sur M, Wall JT, Kaas JH (1984) Modular distribution of neurons with slowly adapting and rapidly adapting responses in area 3b of somatosensory cortex in monkeys. J Neurophysiol 51:724–744.

Talbot WH, Darian-Smith I, Kornhuber HH, Mountcastle VB (1968) The sense of flutter-vibration: comparison of the human capacity with response patterns of mechanoreceptive afferents from the monkey hand. J Neurophysiol 31:301–334.

Theunissen FE, Sen K, Doupe AJ (2000) Spectral-temporal receptive fields of nonlinear auditory neurons obtained using natural sounds. J Neurosci 20:2315–2331.

Vega-Bermudez F, Johnson KO (1999a) SA1 and RA receptive fields, response variability, and population responses mapped with a probe array. J Neurophysiol 81:2701–2710.

Vega-Bermudez F, Johnson KO (1999b) Surround suppression in the responses of primate SA1 and RA mechanoreceptive afferents mapped with a probe array. J Neurophysiol 81:2711–2719.

Vierck CJ, Favorov OV, Whitsel BL (1988) Neural mechanisms of absolute tactile localization in monkeys. Somatosens Mot Res 6:41–61.

Warren S, Hämäläinen HA, Gardner EP (1986) Objective classification of motion- and direction-sensitive neurons in primary somatosensory cortex of awake monkeys. J Neurophysiol 56:598–622.

Weliky M, Kandler K, Fitzpatrick D, Katz LC (1995) Patterns of excitation and inhibition evoked by horizontal connections in visual cortex share a common relationship to orientation columns. Neuron 15:541–552.

Yoshioka T, Gibb B, Dorsch AK, Hsiao SS, Johnson KO (2001) Neural coding mechanisms underlying perceived roughness of finely textured surfaces. J Neurosci 21:6905–6916.

Yoshioka T, Lawson JJ, Denchev P, Vega-Bermudez F, Johnson KO (2002) Spatiotemporal receptive fields in SI cortex of the alert monkey. Soc Neurosci Abstr 28:650.8.